

Coherent population trapping and polarization fluctuations: The independent-modulator approximation for coherent-population-trapping line shapes

M. Huang, T. U. Driskell, and J. C. Camparo

Physical Sciences Laboratories, The Aerospace Corporation, PO Box 92957, Los Angeles, California 90009, USA

(Received 27 February 2013; published 31 May 2013)

In order to understand how stochastic processes enter and influence coherent atomic dynamics, we have studied the behavior of a Λ system under random polarization variations. Polarization, in addition to amplitude and phase, is a defining feature of a classical vector field. However, to date there has been little study of how quantum systems respond to temporal variations of polarization, even though this problem has practical implications. In our work, we generate a Bernoulli sequence of random polarization changes, and we then examine the average ^{87}Rb coherent-population-trapping (CPT) line shape induced by this stochastic field. To quantitatively conceptualize our results, we have developed an independent-modulator approximation (IMA) theory for CPT line shapes induced by stochastic-polarization fields. The IMA theory is based on the idea that a power spectrum can be understood as a probability distribution of Fourier modulation frequencies. We compare the IMA theory with our experimental results, finding quite good agreement when the polarization correlation time is less than or equal to the CPT dephasing time, which is the regime of primary experimental and technological interest. The utility of the IMA theory lies in its intuitive nature, which we believe has merit for guiding experimentalists' general understanding of stochastic fields and quantum systems.

DOI: [10.1103/PhysRevA.87.053419](https://doi.org/10.1103/PhysRevA.87.053419)

PACS number(s): 32.80.Xx, 32.70.Jz, 82.53.Kp, 32.80.Wr

I. INTRODUCTION

Motivated by the development of the chip-scale atomic clock [1,2] and the chip-scale atomic magnetometer [3], the field of ultraminiature atomic physics (UAP) has grown rapidly over the past decade. In brief, UAP is precision spectroscopy (typically optical-pumping or magnetic-resonance spectroscopy [4]) aimed at generating and accurately probing atomic interactions over millimeter or smaller scales, while at the same time severely constraining the overall size and power of the measurement system. Given this definition, it would be quite natural to think that the underlying phenomena of UAP are well understood, and that the critical issues center solely on its engineering. However, the constraints of UAP often force the atomic phenomena to take place under physical conditions that are avoided in routine laboratory research, and it is those conditions that bring interesting dimensions to the basic atomic physics.

As an example, for reasons of size and power the light source of choice in UAP is the vertical-cavity surface-emitting laser (VCSEL) [5]. The VCSEL, however, is not an ideal light source for precision spectroscopy. In the first place, the laser has a relatively broad linewidth ($\sim 10^2$ MHz) [6,7], which not only limits spectroscopic resolution, but implies that phase-noise to amplitude-noise conversion cannot be ignored [8,9]. Specifically, a VCSEL's phase fluctuations will produce fluctuations in a vapor's absorption cross section, and these give rise to fluctuations in the transmitted laser intensity (i.e., UAP noise). Additionally, VCSELs can suffer random polarization variations [10]. Not only does this bring modal partition-noise into the UAP field-atom interaction [11], but the rapid change in laser polarization can have a direct bearing on the dynamics of resonant phenomena [12,13]. Consequently, if UAP devices are to achieve their true potential, researchers will need to develop a better understanding of the basic stochastic-field-atom interaction [14].

To be concrete, it is not uncommon for researchers to account for the stochastic nature of a field by simply convolving the field's spectrum with the atom's (monochromatic-field) resonant response. While this "convolution picture" is certainly valid for weak fields and one-photon processes [14], it is completely inadequate for describing atomic dynamics in the presence of strong stochastic fields, or when atoms undergo multiphoton processes. Perhaps the most telling demonstration of this comes from the seminal work of Lecompte *et al.* [15], where eleven-photon ionization of Xe by a randomly fluctuating field was enhanced by a factor of $11!$. The general stochastic-field-atom interaction, however, is actually more subtle and complicated than this classic work would suggest, since one must differentiate phase fluctuations from amplitude fluctuations [16], and both of these from polarization fluctuations [17].

Coherent population trapping (CPT) is of wide use in UAP, and it is essentially a multiphoton process. Consequently, one cannot depend on the convolution picture to adequately describe the influence of the VCSEL's stochastic nature on CPT signals. In the present work, we extend our previous investigations looking at CPT signals in the presence of deterministic polarization variations [18], in order to address the question of CPT signals in the presence of stochastic polarization variations. In the next section, we provide a very brief overview of CPT in the presence of deterministic laser polarization variations and then use that understanding to develop an approximate, but intuitive, theory of CPT driven by a field undergoing stochastic polarization fluctuations: an independent modulator approximation (IMA) theory of CPT. In Sec. III, we describe our experiment to test the theory, and then in Sec. IV we compare the theory's predictions with experiment finding reasonably good agreement. Validation of the IMA theory not only provides insight into the stochastic-field-atom interaction, but will likely prove useful

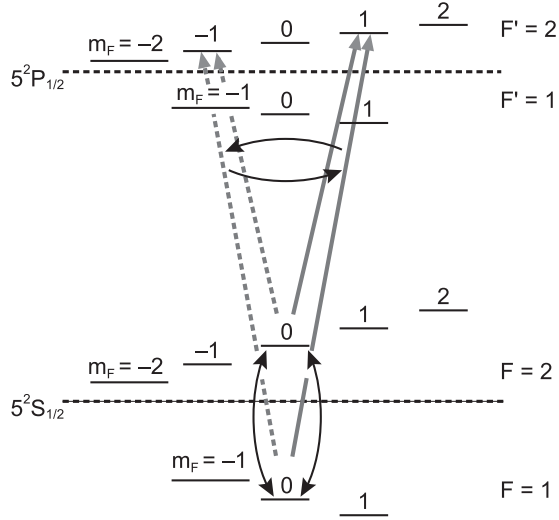


FIG. 1. In the typical CPT experiment with ^{87}Rb , two modes of a laser couple the atom's two $m_F = 0$ $5^2S_{1/2}$ ground-state sublevels to the same excited state; here, the common excited state is the $5^2P_{1/2}$ $|F' = 2, m_{F'} = +1\rangle$ state. The simultaneous coupling creates a coherence in the ground-state, and it is this coherence that is at the heart of the CPT phenomenon. If the laser polarization fluctuates, then the common excited state will momentarily change to $|F' = 2, m_{F'} = -1\rangle$, and this will affect the ground-state coherence.

as a reasonably accurate yet intuitive guide for researchers' thinking.

II. THEORY OF CPT IN THE PRESENCE OF POLARIZATION FLUCTUATIONS

A. CPT and deterministic polarization variations

As illustrated in Fig. 1, realization of the generic CPT phenomenon for the alkali-metal “0-0” hyperfine states requires

$$\frac{\Delta I_{\text{CPT}}(2\delta, \omega)}{I_T(\omega)} = \left\{ \frac{2(I_s/I_c)e^{-\kappa_0(1-2\langle S_z \rangle)}}{1 + 2(I_s/I_c)e^{-\kappa_0(1-2\langle S_z \rangle)}} \right\} \{2\kappa_0 R \eta(1+f)[(f^2 + 2f + 5)R + 8\gamma_2 + 2\kappa_0 R \eta(1+f)]\} \\ \times \left\{ \frac{1}{[(f^2 + 2f + 5)R + 8\gamma_2]^2 + [8(2\delta - \omega)]^2} + \frac{1}{[(f^2 + 2f + 5)R + 8\gamma_2]^2 + [8(2\delta + \omega)]^2} \right\}. \quad (1)$$

Here, $\Delta I_{\text{CPT}}(2\delta, \omega)$ is the change in transmitted intensity due to coherent population trapping, and $I_T(\omega)$ is the magnitude of the transmitted light intensity in the absence of CPT; I_s/I_c is the laser's single sideband-to-carrier intensity ratio, with $2\Delta_s$ the frequency separation between the sidebands: $2\delta \equiv 2\Delta_s - \omega_{\text{hfs}}$; κ_0 is the absorbance of the vapor in the absence of any spin polarization, $\langle S_z \rangle$; R is the photon absorption rate, and γ_2 is the dark dephasing rate of the 0-0 transition (i.e., the dephasing rate in the absence of the field, so that the total dephasing rate, Γ_2 , is $R + \gamma_2$); ω is the polarization modulation frequency; and f is a parameter describing a “filtered-response” approximation for the density matrix when counter-rotating terms cannot be easily ignored (as is done in the secular approximation):

a circularly polarized field [19], so that (for example) the $|F = 1, m_F = 0\rangle$ and $|F = 2, m_F = 0\rangle$ ground-state eigenfunctions only couple to the $|F' = 2, m_{F'} = +1\rangle$ excited state. Of course, the absorption of circularly polarized light transfers angular momentum from the light field to the atomic system, and as a consequence the atomic vapor develops a nonzero electronic spin polarization, $\langle S_z \rangle$ [4,20,21]. Electronic spin polarization plays the role of a *noncoherent* dark state (or equivalently a trapping state), which reduces the alkali vapor density contributing to the *coherent* dark state (i.e., the dark state associated with CPT), and thereby reduces the amplitude of the CPT signal [22].

When the polarization of the field changes abruptly, two different effects take place. First, the discrete laser-polarization change produces a discontinuity in the phase of the ground-state coherence that drives CPT. Consequently, if the polarization is modulated, the coherence is also modulated, and this can lead to a splitting of the CPT signal into a doublet [18]. Additionally, the laser-polarization change leads to a transfer of atomic population among the ground-state Zeeman sublevels as the equilibrium electronic spin polarization changes from $+\langle S_z \rangle$ to $-\langle S_z \rangle$. This latter effect results in a transmitted-laser-intensity transient, which can be nearly an order of magnitude larger than the CPT signal itself [12]. However, if the polarization is modulated fast enough, then the time-averaged transfer of angular momentum from the light field to the atoms approaches zero (i.e., $\langle S_z \rangle \rightarrow 0$), resulting in an overall decrease of population in the trapping state and thereby an overall increase in the CPT signal.

These qualitative considerations have been captured quantitatively in a density-matrix theory describing CPT in the presence of a polarization-modulated field [18], and are summarized by the following closed-form expression for the relative CPT signal:

$f \equiv (R + \gamma_2)/\sqrt{(R + \gamma_2)^2 + 4\omega^2}$. In Eq. (1), the average spin polarization in the vapor $\langle S_z \rangle$ is given by

$$\langle S_z \rangle = \frac{1}{2} \left(\frac{R}{R + \gamma_1} \right) \left[1 - \frac{2}{\pi} \left(\frac{\omega}{R + \gamma_1} \right) \tanh \left(\frac{\pi(R + \gamma_1)}{2\omega} \right) \right], \quad (2)$$

where γ_1 is a “longitudinal” relaxation rate (necessarily an approximate rate, since the system is often described by multiple longitudinal relaxation rates [20]); and η is determined by $\langle S_z \rangle$ through the equation $\eta = (1 - 2|\langle S_z \rangle|)/(2I + 1)$, where I is the nuclear spin. As an illustration, Fig. 2 shows several normalized CPT signals for different modulation frequencies,

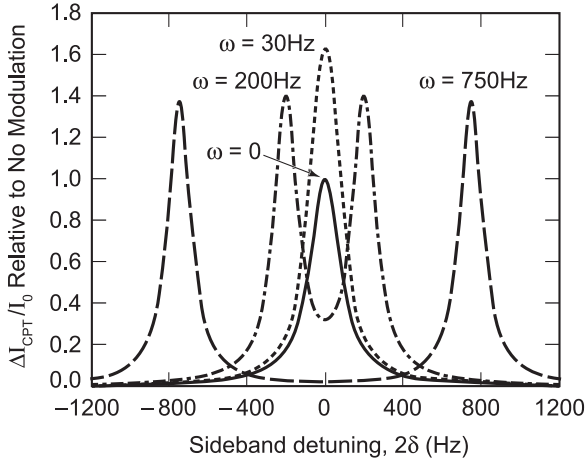


FIG. 2. This figure shows the CPT spectra predicted by Eq. (1) for several values of the polarization modulation frequency ω . Other parameters in the computation include the single sideband-to-carrier intensity ratio, $I_s/I_c = 0.18$, the absorbance, $\kappa_o = 0.57$, the photon absorption rate, $R = 347 \text{ s}^{-1}$, the longitudinal relaxation rate, $\gamma_1 = 57 \text{ s}^{-1}$, and the dephasing rate, $\gamma_2 = 240 \text{ s}^{-1}$.

where it is clear that as ω increases there is an increase in the CPT signal amplitude (due to a decrease in $\langle S_z \rangle$), and then a splitting of the CPT signal into a doublet. Of course, the CPT spectra of Fig. 2 correspond to one well-defined polarization-modulation frequency, while in the present work we are concerned with the shape of CPT signals when the polarization varies randomly.

B. CPT and stochastic polarization variations

Superficially, the response of an atom to a stochastic-polarization field will be akin to that of an atom responding to an amplitude-fluctuating field: in both cases the field's fluctuations enter the atomic dynamics through the Rabi frequency. Of course, there are differences. For one thing, an amplitude-fluctuating field changes the magnitude of the Rabi frequency, whereas a polarization-fluctuating field primarily changes the Rabi frequency's sign. For another, multiple Zeeman states are necessarily involved in the fluctuating polarization case, which is not necessarily true for the fluctuating amplitude case (e.g., the case of a stochastic-amplitude field interacting with a two-level atom). Nevertheless, the similarity highlights the theoretical difficulties of the problem [16], and reinforces the realization that any accurate theoretical description of CPT driven by a polarization-fluctuating field will require numerical solution and likely numerical Monte Carlo simulation [23]. Unfortunately, while accurate numerical solutions/simulations are important (and necessary) for demonstrating that the basic physics of the stochastic-field-atom interaction is well in hand, they are woefully poor at providing intuitive insight. Here, our primary purpose is to develop an *intuitively meaningful* yet reasonably accurate solution to the stochastic-field-atom interaction problem in order to better guide researchers' understanding of the important issues.

To that end, we first note that the power spectrum of a stochastic process, $L(\omega)$, can be interpreted in terms of the likelihood that a Fourier component of the random process will

appear in a long time history of the process. To illustrate this point, as is well known [24] the average power of a stationary random process, $\langle |A|^2 \rangle$, is given by

$$\langle |A|^2 \rangle = \frac{1}{2\pi} \int_{-\infty}^{\infty} L(\omega) d\omega = \int_{-\infty}^{\infty} A_o^2 \left(\frac{L(\omega)}{2\pi \langle |A|^2 \rangle} \right) d\omega \quad (3a)$$

or

$$\langle |A|^2 \rangle = \sum_{i=1}^{\infty} A_o^2 \left(\int_{\omega_i - \delta\omega/2}^{\omega_i + \delta\omega/2} \frac{L(\omega)}{2\pi \langle |A|^2 \rangle} d\omega \right). \quad (3b)$$

Here, A_o is defined as the root-mean-squared amplitude of the random process (i.e., $A_o \equiv \sqrt{\langle |A|^2 \rangle}$), and we have divided the Fourier integral into discrete subintervals of width $\delta\omega$. The point of these apparently trivial manipulations is that Eq. (3b) allows us to interpret A_o as the amplitude of each oscillatory component that appears in a Fourier transform of any *realization* of the random process, and the expression in brackets on the right-hand side of Eq. (3b) as the probability, $P(\omega_i)$, that Fourier frequencies between $\omega_i - \delta\omega/2$ and $\omega_i + \delta\omega/2$ will appear in a random-process realization

$$P(\omega_i) = \frac{1}{2\pi A_o^2} \int_{\omega_i - \delta\omega/2}^{\omega_i + \delta\omega/2} L(\omega) d\omega. \quad (4)$$

If we now ignore the transients that will be induced in the atomic system when the *rate* of polarization fluctuations changes (i.e., when $\omega \rightarrow \omega + d\omega$), then we can make an appeal to the ergodic theorem to write averages over time in terms of an ensemble average over ω . In essence, we are assuming that we can rewrite a long-time average of the stochastic process in terms of a weighted average over “independent” modulation responses of the atom. For obvious reasons, we call this an independent-modulator approximation (IMA) to the stochastic-field-induced atomic dynamics. Clearly, we can expect this approximation to be valid if the correlation time of the stochastic process, Γ_p^{-1} , is much longer than the dephasing time of the atomic system, since in that case (for “well-behaved” random processes) all variations are relatively slow and adiabatically followed by the atomic system. However, we expect that the approximation will become problematic as the correlation time shortens; in particular, we expect the approximation to break down for $\Gamma_p/\Gamma_2 \gg 1$.

Employing the independent-modulator approximation here, we write the CPT line shape in the presence of polarization fluctuations as

$$\frac{\Delta I_{\text{CPT}}(2\delta)}{I_T} \cong \frac{1}{N} \int_{-\infty}^{\infty} L(\omega) \frac{\Delta I_{\text{CPT}}(2\delta, \omega)}{I_T(\omega)} d\omega, \quad (5a)$$

where $L(\omega)$ is the power spectrum of the polarization fluctuations, and N is a normalization factor

$$N \equiv \int_{-\infty}^{\infty} L(\omega) d\omega. \quad (5b)$$

It is important to note that Eq. (5a) is not a convolution: we are not convolving a CPT line shape with the laser spectrum. Rather, we are performing a weighted average of Eq. (1) over polarization modulation frequencies, with the weighting factors defined by the power spectrum of the stochastic polarization fluctuations.

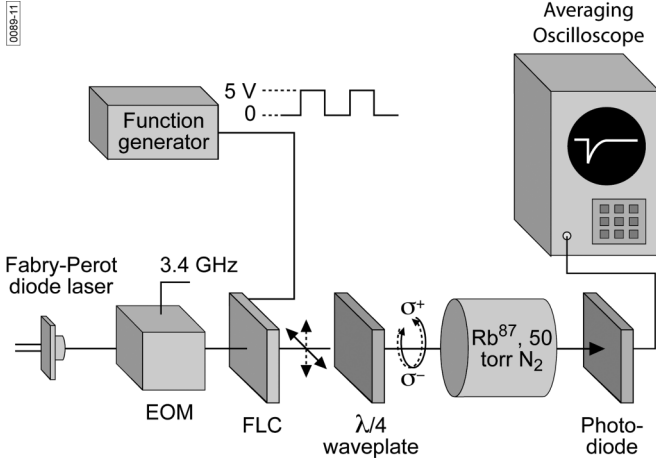


FIG. 3. Block diagram of our experimental arrangement. The Rb cell was maintained at a temperature of 48 °C, corresponding to an alkali density of $\sim 10^{11}$ cm $^{-3}$, and the Rb atoms were contained with a 50 torr N $_2$ buffer gas. The laser light passed through an electro-optic modulator that placed sidebands on the laser at ~ 3.4 GHz. Additionally, though not shown, the light passed through a neutral density filter. In our experiments the single sideband-to-carrier power ratio was 0.18.

III. EXPERIMENT

A. Experimental arrangement

Our experimental arrangement is illustrated in Fig. 3. To generate the Λ -system coherence, we employ a cleaved-facet Fabry-Perot diode laser [25], which does not suffer intrinsic polarization fluctuations. The laser light then passes through an electro-optic modulator (EOM), which places sidebands on the laser at $\pm\Delta_s \cong \pm\omega_{\text{hfs}}/2$ with a single-sideband to carrier intensity ratio (I_s/I_c) of 0.18; here, ω_{hfs} is the ground-state hyperfine transition frequency (i.e., 6834.7 MHz for ^{87}Rb). The beam diameter is 0.6 cm at the entrance to our resonance cell, and the total laser power entering the EOM is 2.5 mW; the intensity of a single sideband I_s in the resonance cell is therefore ~ 1.2 mW/cm 2 . [Though not shown, the light also passes through a neutral density filter (ND) allowing variation of the laser intensity.] The modulated and linearly polarized field then passes through a ferroelectric liquid crystal (FLC) polarization rotator (manufactured by Micron Technology Inc.), which has a bandwidth of 10 kHz and changes the field's linear polarization by ninety degrees depending on an applied voltage. Following this, the field passes through a quarter-wave plate, creating right or left-circularly polarized light, and then into a resonance cell containing isotopically enriched ^{87}Rb and 50 torr of N $_2$ as a buffer gas; using N $_2$, the dominant relaxation mechanism in our system is electron-spin randomization (also known as S -damping) [21]. Pressure broadening of the optical transitions by N $_2$ also implies that the excited-state hyperfine structure is unresolved [26].

Our Pyrex resonance cell is 3.9 cm long with a diameter of 2.2 cm, and for these experiments was maintained at 48 °C with braided heating wire wrapped around the cell body; the absorbance of the vapor, κ_0 , was measured as 0.57: $I(L) = I_0 e^{-\kappa_0 L}$ with I_0 defined as $I_s 10^{-\text{ND}}$ (i.e., the sideband intensity after passing through the neutral density filter). The resonance

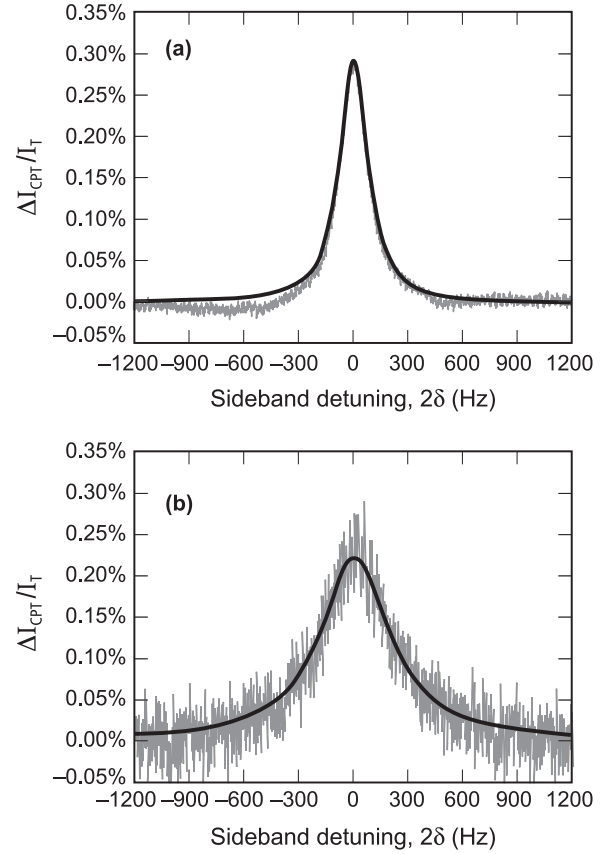


FIG. 4. (a) An example of our CPT line shapes in the absence of stochastic polarization variations (i.e., $p = 0$); the data was taken with a relative light intensity, I_o/I_s , of 0.06, and the solid line through the data is a Lorentzian least-squares fit: Amplitude = 0.28% and $\Delta\nu_{\text{HWHM}} = 576$ s $^{-1}$. (b) An example of our CPT line shape in the presence of stochastic polarization variations (i.e., $p = 0.3$): $\Gamma_p = 916$ s $^{-1}$; the data was taken with a relative light intensity, I_o/I_s , of 0.06, and the solid line through the data is a Lorentzian least-squares fit: Amplitude = 0.22% and $\Delta\nu_{\text{HWHM}} = 1480$ s $^{-1}$.

cell was located in a set of three mutually perpendicular Helmholtz coils with a diameter of 66 cm [27]: two pairs cancelled out the Earth's magnetic field, while the third provided a quantization axis for the atoms along the laser beam's propagation direction (i.e., $B_z = 0.5$ gauss).

Figure 4(a) shows an example of our CPT line shape in the absence of stochastic polarization fluctuations for a relative light intensity, I_o/I_s , of 6.3×10^{-2} . In our experiments we sweep the sideband frequency detuning, 2δ , at a relatively slow rate (i.e., 2.9 kHz/s), and the entire time to generate one spectral line shape, T , is one second. The solid line through the data is a Lorentzian fit, which has a half-width half-maximum, $\Delta\nu_{1/2}$, of 580 s $^{-1}$ (i.e., 92 Hz).

Figure 5 shows our measured values of $\Delta\nu_{1/2}$ as a function of relative light intensity, and from this data we infer that our intrinsic dephasing rate, γ_2 , is 240 s $^{-1}$, and that the optical excitation rate R is given by $R = 5.64 \times 10^3 (I_o/I_s)$ s $^{-1}$. At our nominal light intensity of $I_o/I_s = 6.3 \times 10^{-2}$, which maximizes the relative CPT signal in the absence of polarization fluctuations (and is employed throughout these experiments), we therefore have $R = 347$ s $^{-1}$ and

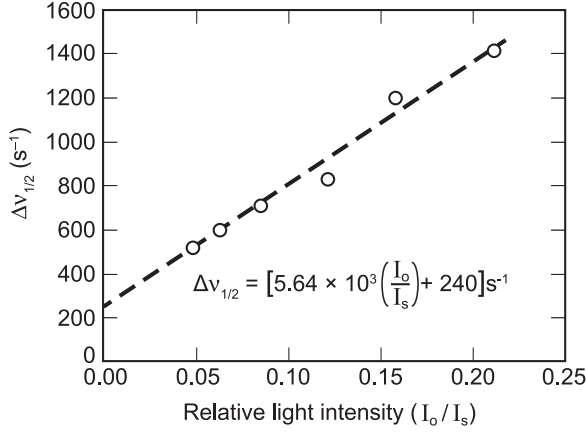


FIG. 5. Half-width half-maximum, $\Delta v_{1/2}$, of the CPT line shape as a function of the relative light intensity. The slope and intercept yield R and γ_2 as reported in Table I.

$\Gamma_2 = 587 \text{ s}^{-1}$. Further, using Eqs. (1) and (2) with $\omega = 0$, and $\Delta I_{\text{CPT}}/I_T = 0.28\%$ for no polarization modulation as shown in Fig. 4(a), we find that $\gamma_1 = 57 \text{ s}^{-1}$. The complete set of parameters required by Eqs. (1) and (2) as determined for our experimental situation are collected in Table I.

B. Stochastic polarization variations

To generate random laser polarization fluctuations, we first divide the sweep time, T , into subintervals δt , with $\delta t = 10^{-3}$ sec, and for each of these subintervals we define a Bernoulli distributed random variable, $x(t)$, that can be either zero or one [28]. Every time a one appears in the Bernoulli process, the function generator controlling the FLC changes: $0 \rightarrow 5 \text{ V}$ or $5 \rightarrow 0 \text{ V}$. In other words, a zero in the Bernoulli process means that the laser field's polarization remains constant, while a one implies that the laser field's polarization changes. Consequently, the number of polarization changes that occur over the entire time period of the sideband frequency sweep is equal to the number of ones that appear in the Bernoulli process over this period. If we define p as the probability for a one to appear in the Bernoulli process, then the mean number of polarization changes during a sweep, $\langle n \rangle$, will be given by $pT/\delta t$, and therefore the average polarization changing rate R_p is just $2\pi \langle n \rangle / T = 2\pi p / \delta t$. Further, the fastest polarization-changing rate we access in our experiment is $2\pi / \delta t = 6283 \text{ s}^{-1}$.

If we now define $\zeta(t)$ as a random process describing the polarization state of the laser: $\zeta = +1 \Rightarrow$ right-circularly polarized light and $\zeta = -1 \Rightarrow$ left-circularly-polarized light,

TABLE I. Experimental parameter values.

Parameter	Value
I_s/I_c	0.18
κ_o	0.57
R	347 s^{-1}
γ_2	240 s^{-1}
$\Gamma_2 = R + \gamma_2$	587 s^{-1}
γ_1	57 s^{-1}

and if we constrain our random polarization changes so that $\zeta(0) = +1$ (i.e., the random process always begins with the laser as right-circularly polarized), then the polarization state of the field at some time t later is just

$$\zeta(t) = (-1)^{k(t)} = \cos[k(t)\pi]. \quad (6)$$

Here, $k(t)$ is a binomial random process [28] given by

$$k(t) = \sum_{i=1}^n x(t_i), \quad (7)$$

where $n = t/\delta t$ (i.e., the number of “draws” of the Bernoulli random variable, or equivalently the number of time steps in the time interval t).

The average value of $\zeta(t)$, $\langle \zeta(t) \rangle$, is just given by

$$\langle \zeta(t) \rangle = \sum_{k=1}^n \cos(k\pi) \binom{n}{k} p^k (1-p)^{n-k} = (1-2p)^{t/\delta t}, \quad (8)$$

where $\binom{n}{k}$ is a binomial coefficient. Clearly, with $p < 1.0$ the mean value of the polarization goes to zero as $t \rightarrow \infty$. Here, we shall restrict our considerations to $p \leq 0.5$; not only are these the cases of most interest for UAP, but for $p > 0.5$ Eq. (8) shows that the average value oscillates between right and left-circularly polarized light at each time step. Though the $p > 0.5$ cases may be of interest academically, they add a level of complication to the analysis that is unlikely to be of much practical import to experimentalists.

To compute the power spectrum of the polarization variations, we first compute the correlation function of $\zeta(t)$

$$\zeta(t)\zeta(t \pm \tau) = (-1)^{2k \pm m} = \cos(m\pi), \quad (9)$$

where m is the number of polarization draws in the time interval τ . This, however, is just given by Eq. (8) with n replaced by $m = |\tau|/\delta t$

$$\langle \zeta(t)\zeta(t \pm \tau) \rangle = (1-2p)^{|\tau|/\delta t}. \quad (10)$$

To obtain the power spectrum, we take advantage of the Wiener-Khinchine relations [29]

$$\begin{aligned} L(\omega) &= \int_{-\infty}^{\infty} e^{-i\omega\tau} \langle \zeta(t)\zeta(t \pm \tau) \rangle d\tau \\ &= \int_{-\infty}^{\infty} e^{-i\omega\tau} (1-2p)^{|\tau|/\delta t} d\tau, \end{aligned} \quad (11)$$

which yields

$$\begin{aligned} \frac{L(\omega)}{N} &= -\frac{1}{\pi} \frac{\delta t \ln(1-2p)}{[\ln(1-2p)]^2 + (\omega\delta t)^2} \\ &= -\frac{1}{\pi} \frac{\delta t \ln[1 - (R_p \delta t / \pi)]}{\{\ln[1 - (R_p \delta t / \pi)]\}^2 + (\omega\delta t)^2}. \end{aligned} \quad (12)$$

The normalized spectrum of polarization fluctuations is thus a Lorentzian with a correlation time, Γ_p^{-1} , equal to $-\delta t / \ln(1-2p)$; this is shown in Fig. 6 for several values of p given $\delta t = 10^{-3}$ sec. Note that for $2p \ll 1$, $\Gamma_p \cong 2p/\delta t$.

Figure 4(b) shows an example of a CPT line shape in the presence of our stochastic polarization fluctuations. For this particular case, $\Gamma_p = 916 \text{ s}^{-1}$ (i.e., $p = 0.3$). Comparison with Fig. 4(a) shows that the stochastic polarization fluctuations have led to a decrease in the CPT amplitude (i.e.,

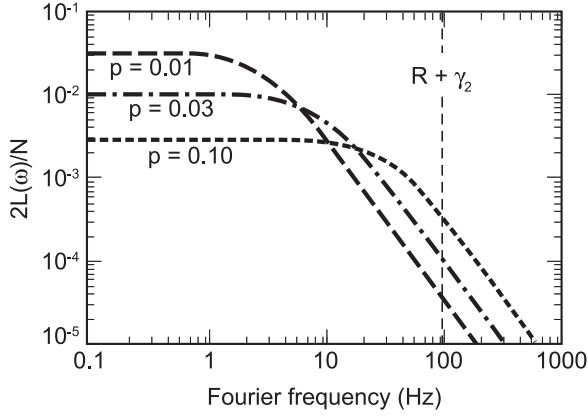


FIG. 6. $L(\omega)/N$ for several values of the probability of polarization changing per time step, p , and with δt taken as 10^{-3} second.

$\Delta I_{\text{CPT}}/I_T = 0.22\%$), and a significant broadening of the CPT line shape (i.e., $\Delta\nu_{1/2} = 1480 \text{ s}^{-1}$). Nevertheless, we find that the stochastic CPT line shape is still well described by a Lorentzian.

IV. RESULTS AND COMPARISON WITH THEORY

Figure 7 shows several examples of our normalized CPT line shapes with a polarization-fluctuating field: (a) $\Gamma_p = 223 \text{ s}^{-1}$ ($p = 0.1$ and $\Gamma_p/\Gamma_2 = 0.38$), (b) $\Gamma_p = 511 \text{ s}^{-1}$ ($p = 0.2$ and $\Gamma_p/\Gamma_2 = 0.87$), and (c) $\Gamma_p = 1609 \text{ s}^{-1}$ ($p = 0.4$ and $\Gamma_p/\Gamma_2 = 2.7$). The solid black line through the data is the CPT line shape predicted by our IMA theory using the parameters of Table I, while the dashed line in the graphs is the CPT line shape in the absence of polarization fluctuations. Without any free parameters, the IMA theory does a surprisingly good job predicting the stochastic-field CPT line shapes up to $\Gamma_p/\Gamma_2 \cong 0.9$. For short correlation times (i.e., $\Gamma_p/\Gamma_2 \geq 1$), the IMA theory still does a credible job, especially with regard to the overall broadening of the CPT line shape and its behavior in the wings. It does, however, predict a doublet structure for the CPT line shape that is not observed experimentally (at least not within the signal-to-noise ratio). Part of the value of the IMA theory, however, is not just in terms of its predictive capabilities, but in terms of its interpretive capabilities. Specifically, in the IMA theory broadening is seen to come from those Fourier components in the random process that produce a slitting of the CPT line shape as illustrated in Fig. 2.

Figure 8 shows the CPT linewidth, $\Delta\nu_{1/2}$, as a function of Γ_p , while Fig. 9 shows the relative amplitude of the CPT line shape, ΔI_{CPT} , as a function of Γ_p (i.e., we normalize ΔI_{CPT} to its value in the absence of polarization noise). As suggested by the data of Fig. 7, Fig. 8 provides further evidence that the IMA theory does a reasonably good job in predicting the CPT linewidth, having an error of less than 20% for the conditions shown in the figure. Interestingly, a better predictor of the CPT linewidth over this polarization-bandwidth range is the simple empirical formula, $\Delta\nu_{1/2} = \Gamma_p + \Gamma_2$, though it lacks theoretical justification.

For the amplitude of the CPT line shapes shown in Fig. 9, the IMA theory actually does a very good job: the CPT amplitude reaches its maximum value for $\Gamma_p/\Gamma_2 \cong 0.25$, and

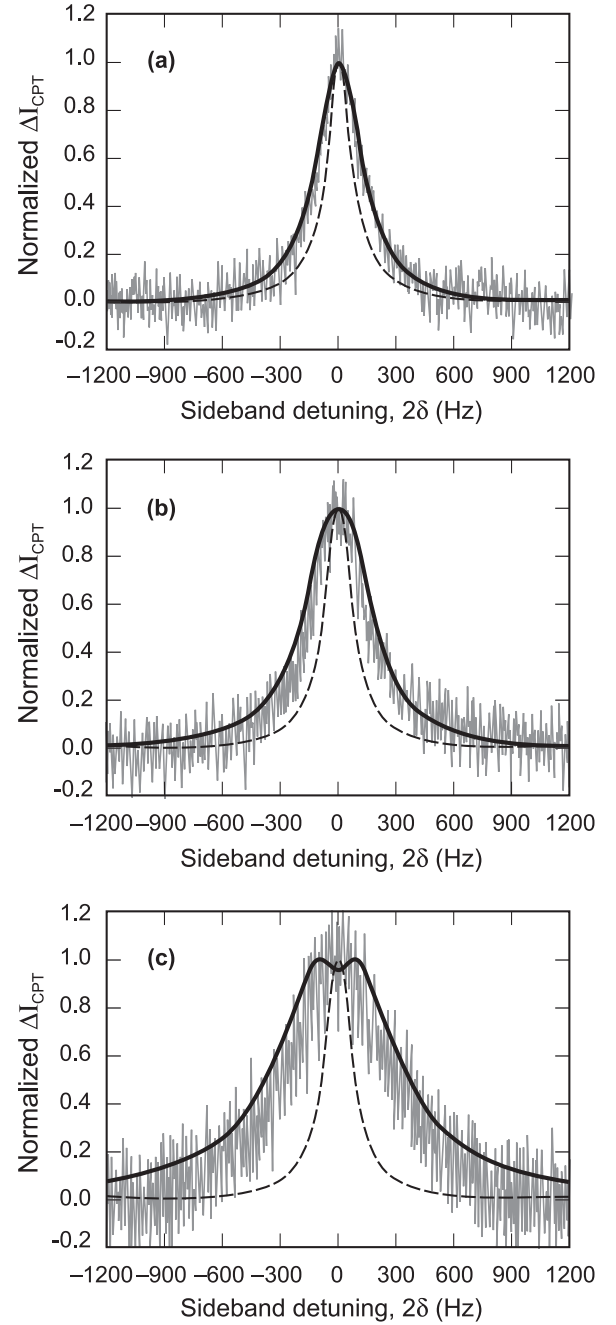


FIG. 7. Comparison between the independent-modulator approximation (IMA) theory of CPT line shapes driven by a polarization-fluctuating field and experiment: (a) $p = 0.1$, $\Gamma_p = 223 \text{ s}^{-1}$, $\Gamma_p/\Gamma_2 = 0.38$; (b) $p = 0.2$, $\Gamma_p = 511 \text{ s}^{-1}$, $\Gamma_p/\Gamma_2 = 0.87$; (c) $p = 0.4$, $\Gamma_p = 1609 \text{ s}^{-1}$, $\Gamma_p/\Gamma_2 = 2.7$. The solid black line through the data is the CPT line shape predicted by our IMA theory using the parameters of Table I, while the dashed line in the graphs is the CPT line shape in the absence of polarization fluctuations.

the amplitude increase is about 60%. Employing the IMA theory for interpretation, we see that the amplitude increase of the CPT signal comes from fast Fourier components of the random process destroying the vapor's electronic spin polarization (i.e., decreasing the population density in the trapping state) as illustrated in Fig. 2.

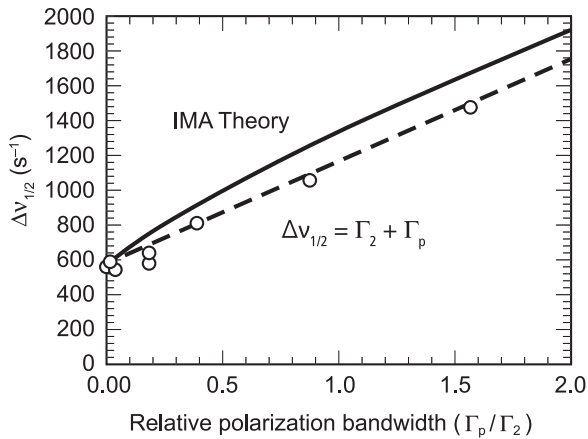


FIG. 8. CPT line widths, $\Delta v_{1/2}$, as a function of the bandwidth of the polarization fluctuations, Γ_p . The solid black line is the prediction from the IMA theory, while the dashed line corresponds to the simple empirical equation $\Delta v_{1/2} = \Gamma_2 + \Gamma_p$.

V. SUMMARY

In this work, we have experimentally investigated the line shapes of CPT signals for a Λ system, when the optical field producing the lower-level coherence undergoes random polarization variations. We find that as the bandwidth of the polarization fluctuations, Γ_p , increases, so too does the CPT linewidth. Additionally, as Γ_p increases the CPT amplitude first increases and then decreases; the maximum CPT amplitude is achieved for $\Gamma_p/\Gamma_2 \sim 0.25$ with Γ_2 the CPT dephasing rate.

To explain our results both quantitatively and intuitively, we developed an independent-modulator approximation (IMA) theory of stochastic-field CPT line shapes. Essentially, this theory assumes that each Fourier component in a realization of a random process produces a static CPT line shape (i.e., the CPT line shape that would be produced by a

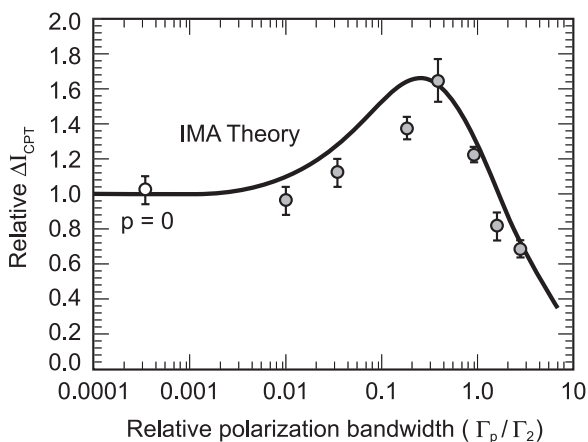


FIG. 9. The amplitude of the CPT signal (normalized to its value for $p = 0$: no polarization noise) as a function of the bandwidth of the polarization fluctuations, Γ_p . The solid black line is the prediction from the IMA theory, and the open data point actually corresponds to $p = 0$. (To place the $p = 0$ data point on this logarithmic plot, we set Γ_p equal to one tenth its smallest possible value for our experimental conditions: $\Gamma_p = -\ln[1 - 0.2\delta t/T]/\delta t$.)

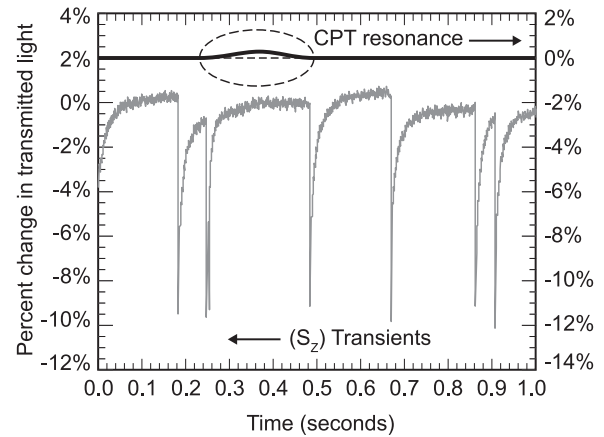


FIG. 10. The change in transmitted light intensity for the CPT signal and the transients induced by the change in electronic-spin polarization, $\langle S_z \rangle$, plotted on the same scale. The $\langle S_z \rangle$ transients are large, and would make an important contribution to CPT-signal noise.

field undergoing deterministic polarization oscillations at the Fourier frequency). The stochastic-field CPT line shape is then obtained by averaging over these static line shapes weighted by the likelihood that a particular modulation frequency will appear in a long-time history of the random process. With this theory, the broadening of CPT line shapes is seen to arise from those Fourier components of the stochastic process that lead to a splitting of the CPT line shape, and the amplitude increase comes from the fast Fourier components of the stochastic process that lead to destruction of electronic-spin polarization.

While the present work has looked into the CPT signal amplitude S and the CPT linewidth, the actual utility of CPT signals in UAP devices is defined by the quality factor $S/(N\Delta v_{1/2})$, where N is the CPT-signal noise. For the typical CPT signal generation process discussed here, where an electronic-spin polarization, $\langle S_z \rangle$, is developed in the vapor, changes in polarization lead to large transients in the transmitted light intensity as atomic population transitions across the Zeeman sublevels. This is illustrated in Fig. 10, where we show the CPT signal ($p = 0$) on the same scale as the $\langle S_z \rangle$ -induced transients in the transmitted light intensity.

UAP device quality factors including CPT-signal noise are a subject for future research. However, it is worth noting that various research groups have devised more sophisticated techniques for CPT signal generation, which essentially eliminate $\langle S_z \rangle$ generation: push-pull optical pumping [30], lin \perp lin excitation [31], and CPT by phase-delayed bichromatic fields [32,33]. The common thread to these techniques is that the field is modulated between right-circularly and left-circularly polarized light at a microwave frequency. As a consequence, while no net angular momentum is transferred to the vapor (i.e., the noncoherent dark state is eliminated), the coherent dark state is preserved. For these more sophisticated techniques, it is quite likely that the stochastic polarization fluctuations considered here would have relatively little effect on the CPT signal's noise, so that our results regarding S and $\Delta v_{1/2}$ would likely apply directly to UAP devices employing those techniques. We intend to explore CPT signals and polarization noise for these other CPT signal generation procedures in future work.

ACKNOWLEDGMENTS

This work was supported under The Aerospace Corporation's Sustained Experimentation and Research for Program

Applications (SERPA) effort, funded by US Air Force Space and Missile Systems Center under Contract No. FA8802-09-C-0001.

-
- [1] S. Knappe, V. Shah, P. D. D. Schwindt, L. Hollberg, J. Kitching, L.-A. Liew, and J. Moreland, *Appl. Phys. Lett.* **85**, 1460 (2004).
- [2] R. Lutwak, J. Deng, W. Riley, M. Varghese, J. Leblanc, G. Tepolt, M. Mescher, D. K. Serkland, K. M. Geib, and G. M. Peake, in *Proc. 36th Annual Precise Time and Time Interval (PTTI) Systems and Applications Meeting* (U. S. Naval Observatory, Washington DC, 2004), pp. 339–354.
- [3] P. D. D. Schwindt, S. Knappe, V. Shah, L. Hollberg, J. Kitching, L.-A. Liew, and J. Moreland, *Appl. Phys. Lett.* **85**, 6409 (2004).
- [4] L. C. Balling, in *Advances in Quantum Electronics*, edited by D. W. Goodwin, Vol. 3 (Academic Press, New York, 1975), pp. 1–167.
- [5] D. K. Serkland, K. M. Geib, G. M. Peake, R. Lutwak, A. Rahed, M. Varghese, G. Tepolt, and M. Prouty, in *Vertical-Cavity Surface-Emitting Lasers IX*, Proc. of SPIE, Vol. 6484, edited by K. D. Choquette and J. K. Guenter, 648406 (SPIE - The International Society for Optical Engineering, Bellingham, WA, 2007).
- [6] W. Schmid, C. Jung, B. Weigl, G. Reiner, R. Michalzik, and K. J. Ebeling, *IEEE Photonics Technol. Lett.* **8**, 1288 (1996).
- [7] M. B. Willemsen, A. S. van de Nes, M. P. van Exter, and J. P. Woerdman, *J. Appl. Phys.* **89**, 4183 (2001).
- [8] J. C. Camparo and J. G. Coffer, *Phys. Rev. A* **59**, 728 (1999).
- [9] J. G. Coffer, M. Anderson, and J. C. Camparo, *Phys. Rev. A* **65**, 033807 (2002).
- [10] J. Kaiser, C. Degen, and W. Elsässer, *J. Opt. Soc. Am. B* **19**, 672 (2002).
- [11] M. Huang, J. G. Coffer, and J. C. Camparo, *Opt. Commun.* **265**, 187 (2006).
- [12] M. Huang, J. G. Coffer, and J. C. Camparo, *J. Phys. B* **43**, 135001 (2010).
- [13] A. Shevchenko, M. Kaivola, and J. Javanainen, *Phys. Rev. A* **73**, 035801 (2006).
- [14] J. Camparo, in *Proc. 7th Symposium Frequency Standards and Metrology*, edited by L. Maleki (World Scientific, Singapore, 2009), pp. 109–117.
- [15] C. Lecompte, G. Mainfray, C. Manus, and F. Sanchez, *Phys. Rev. A* **11**, 1009 (1975).
- [16] A. T. Georges and P. Lambropoulos, *Phys. Rev. A* **20**, 991 (1979).
- [17] R. H. Wentworth, *Phys. Rev. A* **23**, 2525 (1981).
- [18] M. Huang and J. C. Camparo, *Phys. Rev. A* **85**, 012509 (2012).
- [19] F. Levi, A. Godone, J. Vanier, S. Micalizio, and G. Modugno, *Eur. Phys. J. D* **12**, 53 (2000).
- [20] W. Happer, *Rev. Mod. Phys.* **44**, 169 (1972).
- [21] W. Happer and W. A. Van Wijngaarden, *Hyperfine Interact.* **38**, 435 (1987).
- [22] J. Vanier, M. W. Levine, D. Janssen, and M. Delaney, *Phys. Rev. A* **67**, 065801 (2003).
- [23] X. Ling, K. A. Smith, and F. B. Dunning, *Phys. Rev. A* **47**, 480 (1993).
- [24] P. Beckmann, *Probability in Communication Engineering* (Harcourt, Brace & World, New York, 1967), Chap. 6.
- [25] J. Camparo, *Contemp. Phys.* **25**, 443 (1985).
- [26] M. D. Rotondaro and G. P. Perram, *J. Quant. Spectrosc. Radiat. Transfer* **57**, 497 (1997).
- [27] J. H. Moore, C. C. Davis, and M. A. Coplan, *Building Scientific Apparatus* (Addison-Wesley, London, 1983), Chap. 5.
- [28] W. B. Davenport, *Probability and Random Processes: An Introduction for Applied Scientists and Engineers* (McGraw-Hill, New York, 1970), Chap. 9.
- [29] F. Reif, *Fundamentals of Statistical and Thermal Physics* (McGraw-Hill, New York, 1965), Chap. 15.
- [30] Y.-Y. Jau, E. Miron, A. B. Post, N. N. Kuzma, and W. Happer, *Phys. Rev. Lett.* **93**, 160802 (2004).
- [31] T. Zanon, S. Guerandel, E. de Clercq, D. Holleville, N. Dimarcq, and A. Clairon, *Phys. Rev. Lett.* **94**, 193002 (2005).
- [32] M. Rosenbluh, V. Shah, S. Knappe, and J. Kitching, *Opt. Express* **14**, 6588 (2006).
- [33] V. Shah, S. Knappe, P. D. D. Schwindt, V. Gerginov, and J. Kitching, *Opt. Lett.* **31**, 2335 (2006).